microLife, 2024, **5**, uqae021
DOI: 10.1093/femsml/uqae021
Advance access publication date: 15 October 2024
Research Article

Pyoverdine–antibiotic combination treatment: its efficacy and effects on resistance evolution in *Escherichia coli*

Vera Vollenweider*, Flavie Roncoroni, Rolf Kümmerli*

Department of Quantitative Biomedicine, University of Zurich, Winterthurerstrasse 190, 8057 Zurich, Switzerland
*Corresponding authors. Vera Vollenweider, Department of Quantitative Biomedicine, University of Zurich, Winterthurerstrasse 190, 8057 Zurich, Switzerland. E-mail: vera.vollenweider@uzh.ch; Rolf Kümmerli, Department of Quantitative Biomedicine, University of Zurich, Winterthurerstrasse 190, 8057 Zurich, Switzerland. E-mail: rolf.kuemmerli@uzh.ch
Editor: [Carmen Buchrieser]

Abstract

Antibiotic resistance is a growing concern for global health, demanding innovative and effective strategies to combat pathogenic bacteria. Pyoverdines, iron-chelating siderophores produced by environmental *Pseudomonas* spp., present a novel class of promising compounds to induce growth arrest in pathogens through iron starvation. While we previously demonstrated the efficacy of pyoverdines as antibacterials, our understanding of how these molecules interact with antibiotics and impact resistance evolution remains unknown. Here, we investigated the propensity of three *Escherichia coli* strains to evolve resistance against pyoverdine, the cephalosporin antibiotic ceftazidime, and their combination. We used a naive *E. coli* wildtype strain and two isogenic variants carrying the $bla_{\text{TEM-1}}$ β-lactamase gene on either the chromosome or a costly multicopy plasmid to explore the influence of genetic background on selection for resistance. We found that strong resistance against ceftazidime and weak resistance against pyoverdine evolved in all *E. coli* variants under single treatment. Ceftazidime resistance was linked to mutations in outer membrane porin genes (*envZ* and *ompF*), whereas pyoverdine resistance was associated with mutations in the oligopeptide permease (*opp*) operon. In contrast, ceftazidime resistance phenotypes were attenuated under combination treatment, especially for the *E. coli* variant carrying $bla_{\text{TEM-1}}$ on the multicopy plasmid. Altogether, our results show that ceftazidime and pyoverdine interact neutrally and that pyoverdine as an antibacterial is particularly potent against plasmid-carrying *E. coli* strains, presumably because iron starvation compromises both cellular metabolism and plasmid replication.

Keywords: combination treatment; pyoverdine; antimicrobial resistance; experimental evolution; plasmid; *E. coli*

Introduction

Antibiotic-resistant bacteria pose a significant global health problem with estimates predicting 10 million annual deaths attributable to antimicrobial resistance by 2050 (Ventola 2015, Murray et al. 2022). Consequently, there is an urgent need for new and more sustainable approaches to effectively control pathogens and to counteract the emergence and spread of resistance (Bell and MacLean 2018, Monserrat-Martinez et al. 2019, Rezzoagli et al. 2020). While several alternative approaches to antibiotics are under investigation (e.g. phage therapy, antibacterial peptides, and antivirulence approaches) (Wale et al. 2017, Ghosh et al. 2019, Rezzoagli et al. 2020, Xu et al. 2020, Suh et al. 2022, Uyttebroek et al. 2022), we have previously shown that siderophores from environmental bacteria can have strong inhibitory effects on opportunistic human pathogens through the induction of iron limitation (Vollenweider et al. 2024).

Particularly, we found that pyoverdines from environmental *Pseudomonas* spp. show a great structural diversity and high iron-chelation properties and are thus able to induce iron starvation and growth arrest in difficult-to-treat pathogens such as *Acinetobacter baumannii* and *Staphylococcus aureus* (Vollenweider et al. 2024). Furthermore, we observed that pyoverdine treatment improved the survival of infected *Galleria mellonella* host larvae, while having minimal negative effects on mammalian cell lines and erythrocytes (Vollenweider et al. 2024). Finally, we found low levels of resistance emerging in pathogens exposed to the pyoverdine treatment compared to a conventional antibiotic (Vollenweider et al. 2024).

While pyoverdines (or synthesized derivates) could become potential novel antibacterials, one important aspect that needs closer examination is how pyoverdine treatment interacts with antibiotics and how combination treatment affects selection for antibiotic resistance. Combination treatments are well-established in clinical settings and have been proven successful against *Mycobacterium tuberculosis* infections (Ginsberg and Spigelman 2007, Sacchettini et al. 2008), HIV infections (Richman 2001, Lennox et al. 2009), and *Plasmodium falciparum* malaria infections (Malenga et al. 2005). Here, we explored the efficacy and evolutionarily sustainability of combination therapy involving pyoverdine by using experimental evolution with the model pathogen *Escherichia coli*. Specifically, we subjected this pathogen to either pyoverdine 3G07 (one of the most potent pyoverdines against a range of pathogens; Vollenweider et al. 2024; Fig. S1), ceftazidime (a cephalosporin antibiotic), or a combination of the two.

Additionally, we asked whether the genetic background of the pathogen influences the selection for resistance. We were particularly interested in whether the carriage of elements conferring resistance to other antibiotics affects resistance evolution against pyoverdine and/or ceftazidime. To address this question, we used three different *E. coli* strains (San Millan et al. 2016). We took

Received 23 April 2024; **revised** 18 September 2024; **accepted** 13 October 2024

wildtype *E. coli* MG1655 (MG) as the naive susceptible strain. We further used two isogenic MG variants that both carried the β-lactamase gene bla_{TEM-1}, conferring resistance to β-lactams, such as ampicillin, but not against ceftazidime. One of the strains harboured the bla_{TEM-1} resistance gene on the chromosome (MGc), while the other one carried the same gene on a small multicopy plasmid (MGp). Carrying resistance elements is typically associated with fitness costs and the relative costs of resistance may differ between chromosomal and plasmid-based variants. Plasmids can be costly in the absence of antibiotics because they often contain many genes beyond those involved in resistance, including genes for plasmid replication and maintenance (Rankin et al. 2011, Baltrus 2013). Chromosomally integrated resistance elements should be less costly as long as they do not affect the expression of other genes encoding critical cellular functions (Alekshun and Levy 2007, Vogwill and MacLean 2015). Here, we tested whether these differential costs affect the evolution of resistance against pyoverdine 3G07 and ceftazidime single and combo treatments. We first defined drug efficiency ranges and drug interaction patterns, and then conducted an experimental evolution experiment to test whether the emergence and frequency of resistance phenotypes differ across treatments and strains. Finally, we sequenced the genomes of evolved populations to uncover the genetic basis of putative resistance mechanisms.

Materials and methods

Bacterial strains

We used the *E. coli* K-12 substr. MG1655 (MG) strain and two isogenic constructs containing the β-lactamase gene bla_{TEM-1} either on the chromosome (MGc) or on a nontransmissible multicopy plasmid (MGp) with identical promoters. TEM-1 confers resistance to ampicillin and approximate IC50 concentrations of 0.5 mg/l, 42 mg/l, and 7169 mg/l were calculated for MG, MGc, and MGp, respectively (see IC50 determination below). The plasmid (5369 bp) furthermore contains a *gfp* gene under the control of an inducible L-arabinose promoter and is maintained on average at 19 copies per bacterium. All strains were kindly provided by Professor Alvaro San Millan (Centro Nacional de Biotecnología—CSIC, Madrid). The construction of MGc and MGp is described in detail in San Millan et al. (2016). For the single-gene knockout mutant experiments, we used mutants Δ*oppA-D* from the Keio collection (Baba et al. 2006).

Growth conditions and media

Escherichia coli overnight cultures were grown either in 8 ml lysogeny broth (LB; dose–response curves, competition experiments, and experimental evolution assay) in 50 ml tubes or in 200 µl LB in 96-well plates (phenotypic growth assays) at 37°C and 170 rpm agitation. Cultures grown overnight in tubes were washed twice with 0.8% NaCl and adjusted to an optical density at 600 nm (OD_{600}) of 0.1. Cultures from well plates were used directly for experiments. The iron-limited casamino acid (CAA) medium (1% casamino acids, 5 mM $K_2HPO_4 \times 3H_2O$, 1 mM $MgSO_4 \times 7H_2O$, 25 mM HEPES buffer) was used for all experiments. Ceftazidime pentahydrate stocks of 1 mg/ml, ampicillin sodium salt stocks of 10 mg/ml, and pyoverdine stocks of 30 mg/ml were prepared in CAA. We used crudely purified pyoverdines from supernatants of the environmental *Pseudomonas* strain 3G07 (described in detail elsewhere; Vollenweider et al. 2024). Briefly, we grew the strain in 500 ml CAA medium, supplemented with 250 µM of the strong iron-chelator 2,2′-bipyridyl for 120 h at 28°C and shaken at 170 rpm. We then centrifuged the cultures (15 049 × *g*) for 15 min, decanted the supernatant and adjusted its pH to 6 using 1 M HCl. We harvested the pyoverdines by running the supernatant over Amberlite XAD 16-N resins and eluting the pyoverdines with 50% methanol. We lyophilized fractions containing the highest amount of pyoverdines (measured by fluorescence, excitation: 400 nm and emission: 460 nm) and stored it at −20°C. Since we used crude pyoverdine extracts, the absolute concentration of pyoverdine was unknown and thus expressed relative to the highest concentration of 6 mg/ml used. All chemicals were purchased from Sigma-Aldrich (Buchs SG, Switzerland).

Dose–response curves and IC50 calculation

To determine the inhibitory potential of pyoverdine, ceftazidime, and ampicillin, we subjected the three *E. coli* strains to serially diluted crude pyoverdine extracts (highest concentration 6 mg/ml), to ceftazidime (highest concentration 4 mg/l), or to ampicillin [highest concentration 8 mg/ml (MG), 1024 mg/ml (MGc), and 16 384 mg/ml (MGp)]. To this end, bacterial cultures were grown overnight and prepared as described above. 2 µl of diluted culture were then added to a total of 200 µl medium with treatment on a 96-well plate in triplicates. Bacteria grown in CAA without treatment were included in each assay. Plates were incubated at 37°C in a plate reader and the OD_{600} was measured every 15 min for 48 h. We subsequently subtracted the blank and background values caused by the medium and the treatment from the growth values and calculated the area under the growth curve (AUC; integral) using the R package Growthcurver (Sprouffske and Wagner 2016). AUC values were then expressed relative to the untreated controls and plotted for each concentration. Finally, we fitted 5-parameter logistic regressions using the nplr package (Commo and Bot 2016) and extracted the IC50 values.

Competitive fitness assays

To assess the potential cost of carrying antibiotic resistance on plasmids, we evaluated growth of MGp alone or in competition against MG and MGc. Bacteria were cultured overnight in LB and washed as described above. Competitions were initiated with a 1:1 mixture with each competitor at $OD_{600} = 0.05$. The exact initial proportions were determined via flow cytometry using a Cytek Aurora 5 l spectral analyzer (Cytek Biosciences, Amsterdam, The Netherlands) at a low flow rate and maximum mixing speed (1500 rpm) for 2 s prior to measurement at the Cytometry Facility of the University of Zurich. We recorded 50 000 events. We then diluted the cultures further to $OD_{600} = 0.001$ and incubated the competitors alongside monocultures in CAA or in CAA supplemented with 0.5 mg/l ampicillin at 37°C and shaken at 170 rpm for 46 h. After incubation, cultures were diluted in 1× phosphate buffer saline (Gibco, ThermoFisher, Zurich, Switzerland) to $OD_{600} = 0.05$. To distinguish MGp from the competitors, we induced green fluorescent protein (GFP) expression by adding 0.2% L-arabinose for 2 h at room temperature and added propidium iodide (PI, 2 µl of 0.5 mg/ml solution) to distinguish live from dead cells. Upon signal induction, we determined strain proportions with flow cytometry (all events in a 5 µl volume) using a high-throughput plate loader system and the following filters (laser: 488 nm, filter: 530/30, for GFP; laser: 355 nm, filter: 720/29, for PI).

For analysis, we used the software FlowJo (BD Biosciences, Ashland, OR) and followed the same gating strategy for all samples. First, we used forward- and side-scatter height values to separate bacterial cells from background. Within this gate, we excluded any doublings and retained only single cells using the

forward- and side-scatter height and area values, respectively. Next, dead cells were excluded based on PI staining. Finally, we distinguished MGp from competitors by dividing cells into GFP-positive and negative populations. The relative fitness of MGp was then calculated using the formula $\ln(v) = \ln\{[a_{48}\times(1-a_0)]/[a_0\times(1-a_{48})]\}$, where a_0 and a_{48} are the frequencies of MGp at the beginning and at the end of the competition, respectively (Ross-Gillespie et al. 2007). For each competition and treatment, a total of six replicates were measured, and two independent experiments were performed.

Synergy degree of pyoverdine–antibiotic combination treatment

We used the Bliss independence model to calculate the degree of synergy (S) for growth of each *E. coli* strain in the pyoverdine–antibiotic combination treatment (Baeder et al. 2016). We used the formula $S = f(x,0)\times f(0,y) - f(x,y)$, where $f(x,0)$ is the growth (integral) measured under antibiotic exposure at concentration X; $f(0,y)$ is the growth (integral) measured under pyoverdine exposure at concentration Y; and $f(x,y)$ is the growth (integral) measured in the combined treatment at concentration X and Y. If $S = 0$, pyoverdine and antibiotic act independently; $S > 0$ represents synergy, while $S < 0$ indicates antagonism.

Experimental evolution

To determine whether pyoverdine–antibiotic combination treatment can reduce selection for resistance, we experimentally evolved the three *E. coli* strains in single pyoverdine and ceftazidime treatments, in the combination of both and in a no-drug control treatment for 15 transfers. We used rounded values of the calculated IC50 concentrations for the single treatments (relative pyoverdine concentration of 0.16 and 0.4 mg/l for ceftazidime) and combined these concentrations for the combination treatment. We initiated the experiment with six independently evolving lineages per strain and treatment and arranged them diagonally in six 96-well plates. Evolving populations were surrounded by blank wells to reduce the risk of cross-contamination during transfer. Prior to the assay, strains were grown and prepared as described above, and 2 µl of culture were added to a total of 200 µl medium with or without antibacterial treatment. Plates were incubated at 37°C at 170 rpm for 46.5 h before bacterial cultures were diluted 100-fold into fresh treatment. At the end of each cycle, we added glycerol to the old plates at a final concentration of 15% and stored the plates at −80°C.

Phenotypic characterization of evolved populations

We investigated possible resistance evolution after repeated pyoverdine and ceftazidime treatment by comparing the growth of the evolved populations with that of the ancestor. To do so, we prepared overnight cultures of the evolved populations in 96-well plates as described above and then diluted the cultures 1000-fold into fresh treatment. We included six ancestors per strain and treatment, and 18 ancestors in plain medium. Plates were then incubated at 37°C in a plate reader and growth was measured every 15 min for 48 h. For analysis, we first subtracted the blank and background values from the growth data. Next, we calculated the AUC and expressed the values relative to the mean ancestor growth in plain medium. Finally, we calculated the growth difference between the evolved and the ancestors in the same treatment, which allows us to assess the growth gain of the evolved populations compared with the unevolved populations. To determine whether pyoverdine reduced the selection for ceftazidime resistance in the combo treatment, MGp populations that had evolved in the combo treatment were subjected to conditions without pyoverdine, as well as to single treatments of pyoverdine and ceftazidime, and to the combo treatment, following the same procedure described above.

Genomic analyses of evolved populations

For genomic analyses, we selected the four evolved populations with the highest growth gains observed in our phenotypic screen (Fig. 3) for each of the three treatments (pyoverdine, ceftazidime, and combo) for strains MG and MGp. We further included three growth medium-adapted control populations and one ancestor clone per strain. For sequencing, we grew the populations and clones in 12 ml LB at 37°C and 170 rpm and measured their OD_{600} after 6–8 h. When cultures reached an OD_{600} between 0.8 and 1, we pelleted the cultures by centrifugation (7500 × *g*, 3 min), washed them in 0.8% NaCl, centrifuged again, and finally resuspended the pellet in DNA shield buffer (Zymo research). Cultures were then sent to MicrobesNG (Birmingham, United Kingdom) for library preparation and whole-genome sequencing on the Illumina NovaSeq6000 platform (paired-end, 150 base-pair reads, minimum coverage 30x). Adapter sequences were trimmed using Trimmomatic v0.30 (Bolger et al. 2014) with quality cut-off of Q15, reads were aligned to the closest available reference genome using BWA mem (Li and Durbin 2009), de novo assemblies were performed using SPAdes v3.7 (Bankevich et al. 2012), and contigs were annotated with Prokka v1.11 (Seemann 2014). Variants were predicted by using the breseq 0.37.0 pipeline (Barrick et al. 2014, Deatherage and Barrick 2014) using the polymorphism mode and the *E. coli* MG1655 reference genome (NC_000913.3) and pBGT plasmid genome (San Millan et al. 2016). Variants that were present in the ancestral clones relative to the reference sequence were excluded.

Statistical analysis

All statistical analyses were performed in R 4.0.2 (R Core Team 2020) and RStudio version 1.3.1056 (RStudio Team 2020). One-sample *t*-tests were used to compare the relative fitness and the degree of synergy in growth. We used analysis of variance (ANOVA) to test whether evolved populations grew significantly different than the ancestors and adjusted the *P*-values for multiple comparisons using the Tukey HSD test. The same analysis was applied to the experiments involving single-gene knockout mutants.

Results

Pyoverdine and ceftazidime treatments curb the growth of all *E. coli* strains

To confirm the efficacy of pyoverdine 3G07 and ceftazidime against *E. coli* MG1655, we exposed the three MG strains to increasing drug concentrations and assessed their growth performance (Fig. 1). For both treatments we observed conventional dose–response curves, with no growth inhibition at low concentrations, followed by a decrease in bacterial growth at intermediate and high concentrations. There were no differences in the overall dose response (area under the curve) between the three *E. coli* variants (ANOVA for pyoverdine: $F_{2,6} = 0.13$, $P = .8830$; for ceftazidime: $F_{2,9} = 0.80$, $P = .4790$). For pyoverdine, we estimated the following half maximal inhibitory (IC50) concentrations: MG = 0.15, MGc = 0.27, and MGp = 0.17. Note that the absolute pyoverdine concentration cannot be assessed from the crude extracts we used here,

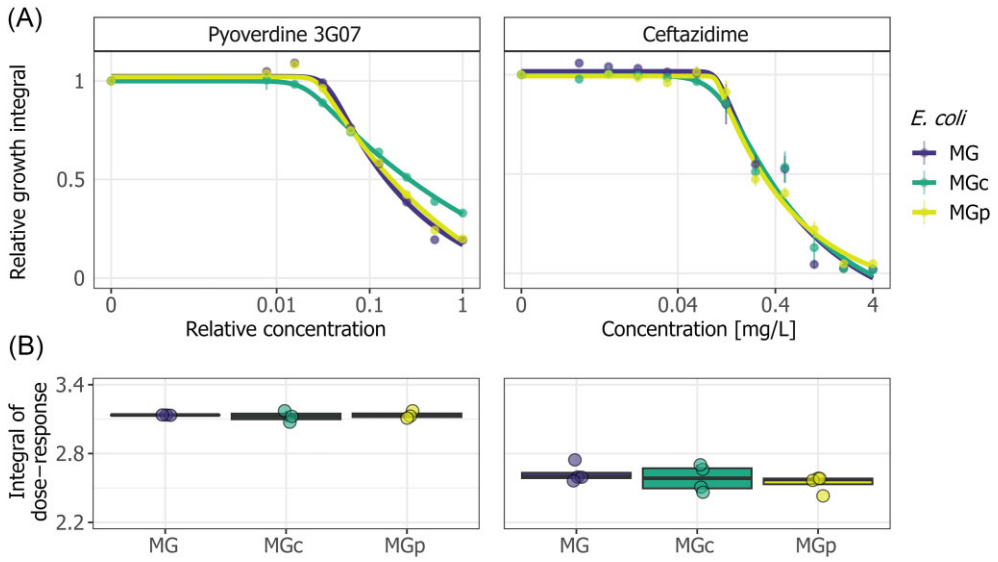

Figure 1. Dose–response curves for *E. coli* strains MG, MGc, and MGp following treatment with pyoverdine 3G07 or ceftazidime. (A) We exposed the three *E. coli* variants, MG (wildtype MG1655), MGc (carrying the *bla*TEM-1 resistance gene on the chromosome), and MGp (carrying the *bla*TEM-1 resistance gene on a multicopy plasmid) to increasing concentrations of pyoverdine 3G07 and ceftazidime and calculated the integral below the growth curves. These values were then scaled relative to the untreated control in CAA medium. Dots and error bars show mean values and standard errors, respectively, across a minimum of six replicates per concentration. Dose–response curves were fitted using 5-parameter logistic regressions. (B) Box plots show the median together with the first and third quartiles and whiskers represent the 1.5x interquartile range. Individual data points show the integrals of the dose–response curves from (A) for the three *E. coli* variants.

Table 1. Interaction (degree of synergy, S) between pyoverdine and ceftazidime treatments based on the Bliss independence model.

	Mean measured growth in…							
Strain	Ceftazidime f(x,0)	Pyoverdine f(0,y)	Combo f(x,y)	Mean degree of synergy (S)[a]	SE	t-value	df	P-value
MG	0.4044	0.4921	0.1538	0.0294	0.0739	0.3979	2	.7291
MGc	0.3998	0.3813	0.1044	−0.0277	0.0574	−0.4823	2	.6772
MGp	0.3434	0.5096	0.1931	0.0446	0.0186	2.4011	2	.1383
Combined	0.3825	0.4670	0.1505	0.0155	0.0297	0.5209	8	.6166

[a]S = f(x,0) x f(0, y)—f(x, y); synergistic S > 0, additive (neutral) S = 0 or antagonistic S < 0 interaction.

and that is why we express concentrations relative to the weighed amount of 6 mg/ml. For ceftazidime, estimates of IC50 concentrations were 0.31 mg/l for MG, 0.32 mg/l for MGc, and 0.29 for MGp, and were highly consistent across the three strains.

Pyoverdine 3G07 and ceftazidime show a neutral interaction

To quantify whether the interaction between pyoverdine 3G07 and ceftazidime is antagonistic, neutral (additive), or synergistic, we used the Bliss model to compare whether the combo treatment is less, equally, or more inhibitory than expected, respectively (Baeder et al. 2016). For this comparison, we used a relative pyoverdine concentration of 0.16 and a ceftazidime concentration of 0.4 mg/l for both single and combo treatments, which displayed intermediate inhibition (Fig. 1). We found that all interaction terms are approximately zero, and when combined across strains, the interaction was not significantly different from the expected value (one-sample *t*-test: $t_8 = 0.52$, $P = .6166$; Table 1). This result suggests that the interaction between pyoverdine 3G07 and ceftazidime is neutral (additive).

Plasmid-based antibiotic resistance entails a fitness cost

Next, we investigated whether carrying a plasmid encoding a resistance gene is associated with fitness costs. To this end, we competed the plasmid-carrying strain MGp against the isogenic strain MG and the chromosomally resistant strain MGc both in medium without and with ampicillin, the antibiotic to which $bla_{\text{TEM-1}}$ confers resistance. For all competitions, we used 0.5 mg/l ampicillin, which represents the IC50 concentration of strain MG (Fig. S2).

In the absence of ampicillin, the fitness of MGp was significantly reduced compared to MG (one-sample *t*-test, $t_5 = -3.15$, $P = .0254$) and MGc ($t_5 = -3.96$, $P = .0107$) (Fig. 2). These results demonstrate that plasmid carriage is associated with fitness costs in the absence of antibiotics. Meanwhile, in the presence of ampicillin, the benefits of carrying a resistance plasmid exceeded its cost, resulting in MGp exhibiting significantly higher fitness compared to the susceptible strain MG ($t_5 = 29.50$, $P < .0001$). Nonetheless, even in the presence of ampicillin, MGp exhibited reduced fitness compared to MGc ($t_5 = -2.72$, $P = .0416$), showing that plasmid-based resistance entails higher costs than chromosomal-based resistance in our system.

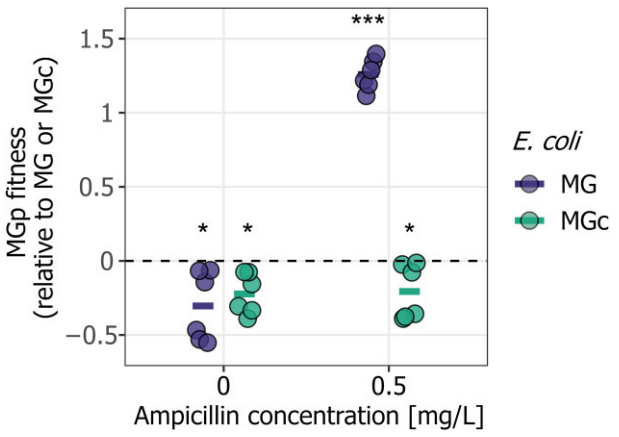

Figure 2. Relative fitness of plasmid-carrying *E. coli* MGp in competition against *E. coli* MG and MGc. We tested whether carrying an antibiotic resistance plasmid has a cost compared to a naive strain (MG) and a strain carrying the resistance gene on the chromosome (MGc). *Escherichia coli* MGp was therefore competed against MG and MGc for 48 h, starting at a 1:1 ratio. The dashed line indicates fitness parity, at which neither of the competing strains has a fitness advantage. Without any antibiotic treatment (0 mg/l ampicillin), MGp had a fitness disadvantage (fitness values <0) compared to MG and MGc, showing the cost of plasmid-based resistance. When treated with 0.5 mg/l ampicillin, MGp experienced highly significant fitness advantages (fitness values >0) compared to MG, and slight significant fitness disadvantages compared to MGc. All data are shown as means ± standard errors across six replicates from two independent experiments. Significance levels are based on one-sample *t*-tests (comparison against the null-line): * $P < .05$; ** $P < .01$; and *** $P < .001$.

Combination treatment reduces selection for resistant phenotypes in *E. coli* MGp

We then conducted an experimental evolution to assess whether *E. coli* strains MG, MGc, and MGp evolve resistance to either pyoverdine 3G07, ceftazidime, or the combo treatment. We propagated six independent populations per condition and strain every other day to fresh medium for 15 transfers (30 days in total). To control for adaptation to the growth medium, we also evolved the three *E. coli* strains in the absence of drugs, resulting in a total of 72 evolving populations (Fig. S3). Subsequently, we subjected the evolved populations from the final transfer to the conditions they evolved in and compared their growth relative to the ancestral wildtypes (Fig. S4) by calculating the difference in growth between the evolved and ancestral populations.

We found that evolved MG populations grew significantly better under pyoverdine, ceftazidime, and the combo treatment compared to the control populations that evolved without antibacterials (global analysis: ANOVA, $F_{3,20} = 51.07$, $P < .0001$; Fig. 3). This suggests that MG populations evolved (at least partial) resistance to pyoverdine, ceftazidime, and the combo treatment. In contrast, evolved MGc populations only showed significantly improved growth under ceftazidime and the combo treatment but not under pyoverdine single treatment (compared to evolved control: ANOVA, $F_{3,20} = 19.6$, $P < .0001$). Finally, the evolved MGp populations grew significantly better only under ceftazidime treatment, but not under pyoverdine or the combo treatment (compared to evolved control: ANOVA, $F_{3,20} = 30.14$, $P < .0001$). These results suggest that MGp evolved resistance to ceftazidime, but not against treatments containing pyoverdine. An alternative explanation is that MGp grew more slowly under treatment such that the number of generations and mutation supply for adaptive evolution might have been reduced in this strain. We found no evidence for this hypothesis as generation times and thus the expected number of mutations did not significantly differ among the ancestral *E. coli* variants neither under pyoverdine ($F_{2,57} = 2.13$, $P = .1290$) nor ceftazidime ($F_{2,33} = 0.22$, $P = .8010$) treatments (Table S1). Taken together, our analyses indicate that the genetic background of the strains influences resistance evolution, and that resistance evolution seems lowest in MGp.

Independent mode of action of pyoverdine hides ceftazidime resistant phenotypes in *E. coli* MGp populations

Given the reduced growth gain in evolved *E. coli* MGp populations in the combo compared to the ceftazidime single treatment, we wondered whether pyoverdine 3G07 can indeed reduce selection for resistance or whether ceftazidime resistance still emerges but remains phenotypically hidden. This could happen due to the independent (additive) inhibitory effect of pyoverdine. To differentiate between these two possibilities, we exposed the MGp ancestor and MGp populations evolved in the combo treatment to single pyoverdine 3G07 and ceftazidime treatments as well as the no-drug control treatment. We monitored their growth for 48 h (Fig. S5) and calculated the growth gain as described above.

We found that the MGp populations evolved in the combo treatment showed significant differences in growth gain when exposed to single treatments (ANOVA, $F_{2,15} = 32.90$, $P < .0001$; Fig. 4). No significant difference in growth gain occurred between the no-treatment control and the pyoverdine treatment (Tukey *post hoc*: $P = .6635$), suggesting low levels of pyoverdine resistance. By contrast, growth gains in MGp populations evolved in the combo treatment were substantial under ceftazidime exposure and significantly higher in the ceftazidime single (mean ± SD: 0.392 ± 0.082) than in the combo (0.283 ± 0.056) treatment ($P = .0207$). This shows that pyoverdine 3G07 does not prevent the evolution of ceftazidime-resistant phenotypes in MGp populations under combo treatment. It supports the notion that the two drugs interact neutrally, making the evolution of resistance for the two drugs independent.

Mutation frequencies of evolved *E. coli* MG and MGp populations

The above growth screen suggests that *E. coli* MG populations developed resistance to both pyoverdine 3G07 and ceftazidime treatments, while *E. coli* MGp specifically acquired resistance to ceftazidime. To link these observed phenotypes to mutational patterns, we sequenced four evolved populations per antibacterial treatment and three no-treatment control populations from the final day of experimental evolution. Overall, we sequenced 30 populations, 15 each for MG and MGp. We excluded mutations present in ancestral clones and focussed on those accumulated during experimental evolution.

In total, we identified 453 and 1221 mutations across all MG and MGp populations, respectively. Mutation frequencies within populations ranged from 5% (our lower cut-off) to 100%. Across all evolution conditions and strains, mutation frequencies exhibited a bimodal distribution: the majority (1371) of mutations occurred at low frequencies (<30%), while a minority (303) occurred at higher frequencies (>30%; Fig. 5A). The low-frequency mutations appeared in intergenic regions (47.8%), pseudogenes (24.9%), coding regions (22.1%), and noncoding regions (5.1%; Table S2). We excluded these low-frequency mutations from further analyses since we argue that many of them might be neutral and subject to drift rather than selection.

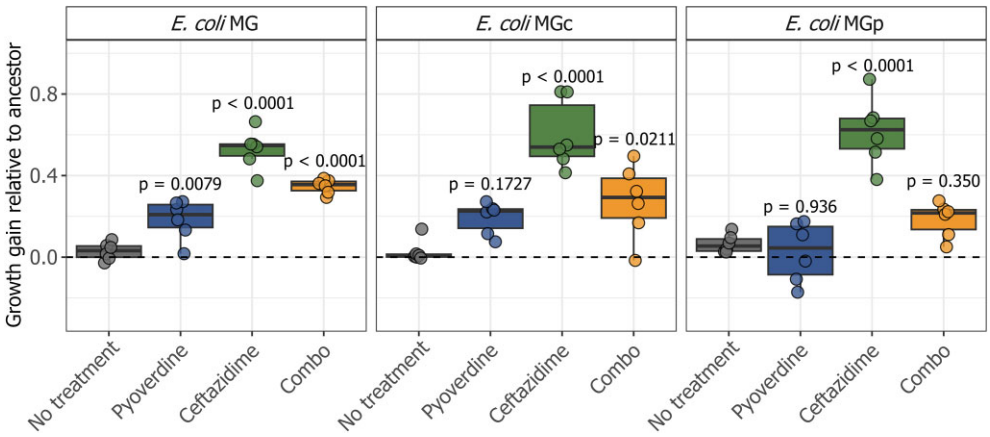

Figure 3. Growth gain of evolved *E. coli* MG, MGc, and MGp populations relative to ancestral populations in the no-treatment control, or the three antibacterial treatments pyoverdine 3G07, ceftazidime, and their combo. We exposed the evolved *E. coli* populations to the conditions in which they evolved in (no-treatment control, pyoverdine 3G07, ceftazidime, and combo treatment). We further exposed the ancestors to the same four conditions. We quantified growth by calculating the integrals under the growth curves, which were then scaled relative to the ancestral growth in plain CAA medium. The difference in growth values was subsequently calculated between evolved and ancestor populations that experienced the same treatment condition. This difference corresponds to the growth gain of evolved populations. Each dot denotes a population and represents the mean value across six replicates. Box plots show the median together with the first and third quartiles and whiskers represent the 1.5x interquartile range. The dotted line represents the ancestral baseline and the *P*-values above antibacterial treatment boxplots indicate the significance levels relative to the no-treatment control (assessed by ANOVA with adjusted *P*-values using the Tukey HSD method, $\alpha = 0.05$).

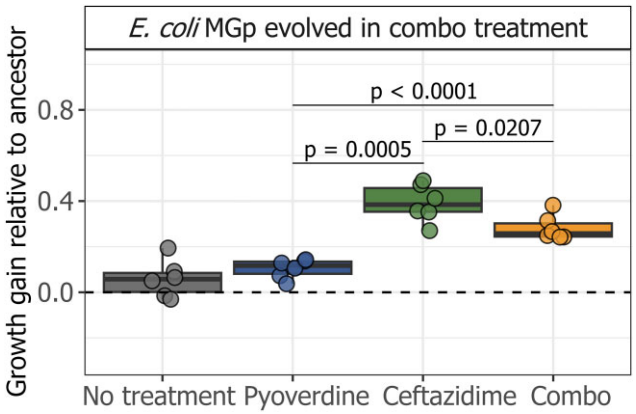

Figure 4. Growth gain of *E. coli* MGp populations evolved in the combo treatment and tested under single pyoverdine 3G07 and ceftazidime treatments. We exposed the six *E. coli* MGp populations that evolved in the combo treatment to single pyoverdine and ceftazidime treatments, as well as to the no-treatment control and the combo treatment in which they evolved. Growth gain is represented by the scaled difference in growth integral between evolved and ancestor populations. Each dot denotes a population and represents the mean value across six replicates. Box plots show the median together with the first and third quartiles and whiskers represent the 1.5x interquartile range. Statistical analysis was performed using ANOVA with adjusted *P*-values using the Tukey HSD method ($\alpha = 0.05$).

Focusing on high-frequency mutations (>30%), we identified single-nucleotide polymorphisms (SNPs) as the most common mutation (135), followed by deletions (97), insertions (50), mobile element insertions (MOB; 20), and amplification (1). Most mutations appeared in intergenic regions (52.5%), followed by coding regions (47.2%) and pseudogenes (0.3%).

Next, we excluded genes with synonymous mutations and genes that mutated in both no-treatment control and antibacterial treatments as they are probably associated with adaptation to the growth medium. After this filtering process, the frequencies of the remaining mutations were similar in the pyoverdine treatment (12 and 15 mutations), the ceftazidime treatment (11 and 12), and the combo treatment (15 and 19 mutations in MG and MGp, respectively), and did not differ between MG and MGp (Fisher's exact test, $P = .9619$).

Comparison of mutational patterns in single and combo treatments

To identify putative key mutations responsible for resistance phenotypes, we compared the number of mutations unique to a particular antibacterial treatment with those shared between treatments. This analysis yielded little overlap in the mutational patterns between treatments (pairwise comparisons) and no mutation occurred in all three treatments (Fig. 5B). However, those mutations that occurred in two treatments reached high frequencies and surfaced in multiple populations, and we thus expect these mutations to be associated with the observed population-level resistance phenotypes. We now go through the list of these mutations and assess their potential association with antibacterial resistance (Table S3).

For ceftazidime single and combo treatments, mutations in the following genes occurred multiple times at high frequencies (in 17 out of 27 cases the frequency was 100%; Table S3): *ompF* (MG = 7/MGp = 7), *envZ* (4/2), bla_{TEM-1} (0/2), and *proQ* (4/1). *OmpF* encodes the outer membrane porin F (Cai and Inouye 2002, Hirakawa et al. 2003), a known entry point for antibiotics. Loss-of-function mutations in *ompF* reduce membrane permeability, leading to increased levels of antibiotic resistance (Vergalli et al. 2020, Masi et al. 2022). Mutations in *envZ* could have a similar effect. EnvZ is a periplasmic protein that senses changes in the environment and controls the phosphorylation state of its cognate response regulator OmpR, which is a repressor of *ompF*. Thus, mutations in *envZ* could result in the down-regulation of *ompF* expression (Cai and Inouye 2002, Hirakawa et al. 2003). Bla_{TEM-1} is the resistance gene introduced in *E. coli* MGp (San Millan et al. 2016) and encodes a beta-lactamase with high activity against ampicillin. In its original form, it has minimal activity against ceftazidime, but mutations can expand its activity range to ceftazidime (Negri et al. 2000, Salverda et al. 2010, Livermore et al. 2015). ProQ is an RNA chaperon involved in the post-transcriptional control of

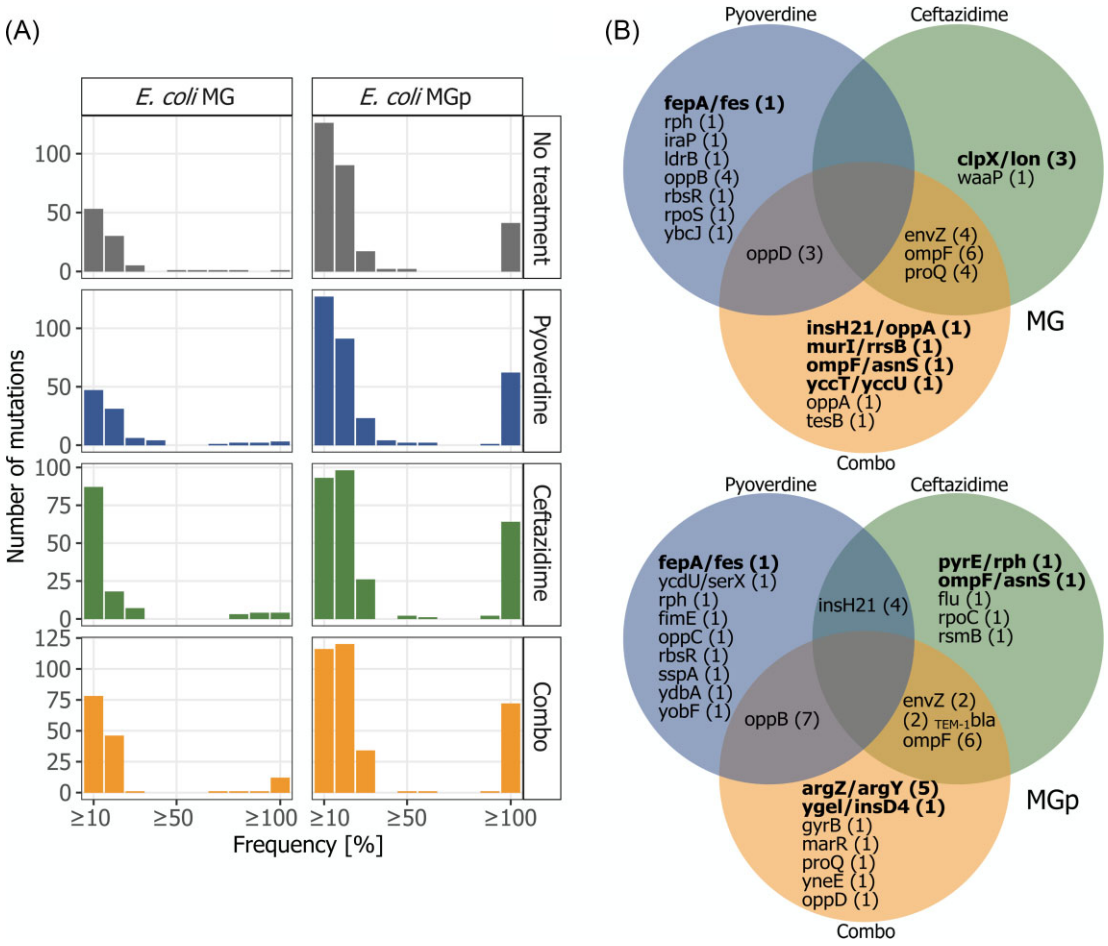

Figure 5. Mutational patterns in *E. coli* MG and MGp after evolution in pyoverdine 3G07, ceftazidime, or the combo treatment. (A) Bimodal distribution of the number of mutations per population of MG and MGp after evolution. In total, 1371 mutations were present at low frequency (<30%), while 303 mutations were present at higher frequency (>30%). (B) Venn diagrams showing the genes unique to or shared between populations evolved in pyoverdine 3G07 (left circle), ceftazidime (right circle), or the combo (center circle) treatment for MG (top) and MGp (bottom). Bold letters indicate mutations in intergenic regions and numbers in brackets indicate the number of independent mutations observed within that region/gene.

ProP levels, which are plasma membrane transporters that sense and respond to osmotic changes (Sheidy and Zielke 2013). Here, it is less clear how mutations in this gene could be involved in ceftazidime resistance.

For the pyoverdine 3G07 single treatment, we identified a SNP in the regulatory region between genes encoding the ferric enterobactin outer membrane transporter FepA (Klebba 2003, Annamalai et al. 2004, Chakraborty et al. 2007) and the ferric enterobactin esterase Fes (Brickman and McIntosh 1992, Schalk and Guillon 2013) in both MG and MGp (Fig. S6). Enterobactin, a high-affinity siderophore produced by *E. coli*, binds iron and is transported by FepA, while Fes catalyses the hydrolysis of the ferric–enterobactin complex in the cytosol (Raymond et al. 2003). Notably, the ferric uptake regulator (Fur) protein-binding site, which is crucial for regulating the response to iron starvation, is situated between FepA and Fes (Pettis et al. 1988, Hunt et al. 1994, Escolar et al. 1998). Consequently, mutations in this region may result in a constant dissociation of Fur and consequently to a constitutive expression of genes related to enterobactin transport and utilization. The upregulation of enterobactin could be beneficial, as this siderophore has higher iron affinity than pyoverdine and could thus alleviate the iron starvation imposed by pyoverdine.

Additionally, we found that mutations in the genes of the *opp*-operon were common (MG/MGp: *oppA* = 1/0, *oppB* = 4/7, *oppC* = 0/1, and *oppD* = 3/1) in populations of the pyoverdine single and combo treatments, reaching high frequencies (mean ± SE, MG: 0.83 ± 0.05; MGp: 0.80 ± 0.08; Table S4). Furthermore, two MGp populations displayed the same 1199 bp deletion of the *insH21* IS5 element, which is located upstream of the *oppABCDF* operon, and one MG population acquired a mutation in the intergenic region of *insH21/oppA*. This operon encodes an oligopeptide importer (Masulis et al. 2020) and the uncovered mutations are likely associated with a loss-of-function (Fig. S7). Since pyoverdine is a modified oligopeptide, we speculate that loss-of-function mutations in the *opp*-operon could potentially prevent the uptake of apo-pyoverdine. A reduction in apo-pyoverdine uptake could prevent this molecule from interfering with intracellular iron homeostasis.

Enhanced growth of *E. coli* Δ*oppA* and Δ*oppB* mutants in pyoverdine 3G07 treatment

While our previous work yielded little evidence for resistance evolution against pyoverdine in other pathogens (*A. baumannii*, *Klebsiella pneumoniae*, and *S. aureus*) (Vollenweider et al. 2024), we here identify the *opp* operon as a potential mutational target conferring a moderate level of pyoverdine resistance. The operon *oppABCDF* consists of five genes, encoding a high affinity oligopeptide ABC transporter system with low specificity (Linton and

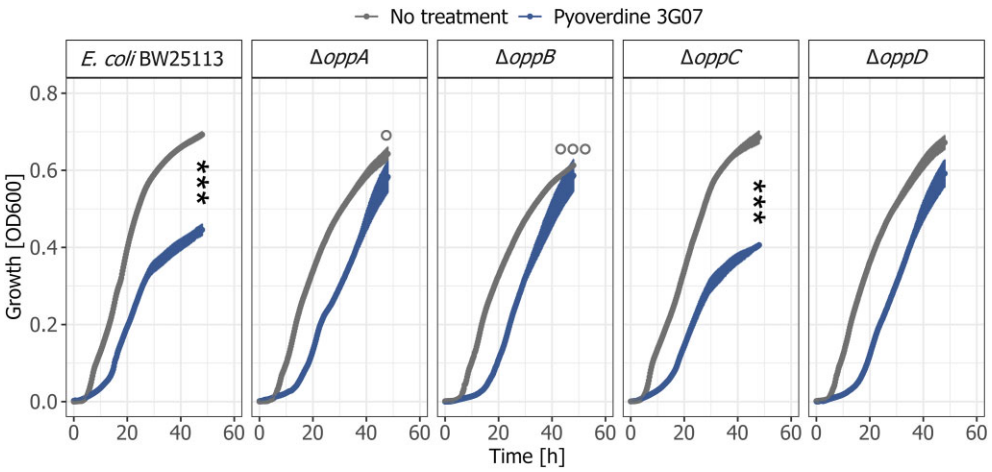

Figure 6. Growth of *E. coli* opp single-gene knockout mutants in the presence and absence of pyoverdine 3G07. Growth kinetics of the *E. coli* knockout mutants Δ*oppA*, Δ*oppB*, Δ*oppC*, Δ*oppD*, and the *E. coli* wildtype BW25113 in growth medium without pyoverdine (upper lines) and with pyoverdine (lower lines) treatment over 48 h. Dots and error bars show mean values and standard errors, respectively, across a minimum of six replicates per treatment from two independent experiments. Significance levels are based on two-sample *t*-tests with $\alpha < 0.05$. Circles represent difference in the end-point growth between the *E. coli* wildtype and the mutants in the no-pyoverdine control (grey lines). Asterisks denote significant differences in the end-point growth between the no-pyoverdine condition and the pyoverdine treatment in each panel. ° and * $P < .05$, °°° and *** $P < .001$.

Higgins 1998, Davidson et al. 2008). OppA is a periplasmic-binding protein, which interacts with the two inner membrane subunits OppBC (Doeven et al. 2004, Klepsch et al. 2011), and the ATP-binding subunits OppDF (Moussatova et al. 2008, Masulis et al. 2020).

To understand whether mutations in the *oppABCDF* operon indeed confer resistance to pyoverdine, we subjected the *E. coli* mutants Δ*oppA*, Δ*oppB*, Δ*oppC*, and Δ*oppD* to pyoverdine 3G07 treatment and compared their growth to that of the parental wildtype BW25133. These mutants originate from the Keio collection (Baba et al. 2006), where the gene of interest is replaced by a kanamycin resistance cassette and thus allows to analyse the effects of loss of gene function.

We first examined whether the lack of a functional Opp-transporter has fitness consequences for *E. coli* in the absence of antibacterial treatment (Fig. 6; grey growth kinetics and circles). We found that growth was reduced in Δ*oppA* (two-sample *t*-test: $t_{10} = 2.46$, $P = .0338$) and Δ*oppB* ($t_{10} = 6.34$, $P = .0001$) compared to wildtype but not in Δ*oppC* ($t_{10} = 0.36$, $P = .7253$) and Δ*oppD* ($t_{10} = 0.98$, $P = .3512$). Overall, growth effects were small suggesting that the Opp-transporter is not essential for *E. coli*.

Next, we tested whether the lack of specific Opp-proteins alleviates the significant growth reduction that pyoverdine treatment has on the wildtype ($t_{10} = -13.76$, $P < .0001$, Fig. 6; blue growth kinetics and asterisk). Indeed, we found that growth yield after 48 h was restored to the level of the no-pyoverdine treatment control in Δ*oppA* ($t_{10} = -1.33$, $P = .2146$) and Δ*oppB* ($t_{10} = -0.61$, $P = .5676$), and to some extent in Δ*oppD* ($t_{10} = -1.97$, $P = .0777$), but not in Δ*oppC* ($t_{10} = -15.06$, $P < .0001$). However, albeit achieving the same yield, the growth of all *opp*-mutants was still substantially slowed down compared to the untreated controls during the early growth phase. These results indicate that mutations in the *opp* operon can confer partial resistance to pyoverdine.

Discussion

We previously demonstrated the potent inhibitory effects of iron-scavenging pyoverdines from environmental *Pseudomonas* spp. on opportunistic human pathogens through the induction of iron limitation (Vollenweider et al. 2024). Building on this work, we here investigated the interaction between pyoverdine 3G07 and the antibiotic ceftazidime to explore how combination therapy affects resistance evolution in three *E. coli* strains. We found neutral drug interactions between pyoverdine and ceftazidime and observed that pyoverdine could not prevent the evolution of ceftazidime resistance in a combination treatment in the naive *E. coli* MG1655 strain (MG) during experimental evolution. In contrast, the presence of pyoverdine reduced ceftazidime resistant phenotypes in *E. coli* MGc (mild effect) and *E. coli* MGp (strong effect), two strains carrying the β-lactamase gene $bla_{\text{TEM-1}}$ (conferring resistance to ampicillin) on the chromosome and a small multicopy plasmid, respectively. Genetic analyses revealed that mutations in the outer membrane porin F (OmpF) and the sensor histidine kinase EnvZ were associated with ceftazidime resistance. Curiously, the frequency of these mutations was similar in both *E. coli* MG and MGp, regardless of whether they were treated with ceftazidime alone or in combination with pyoverdine. This suggests that pyoverdine cannot prevent resistance evolution *per se*, but simply represses the ceftazidime resistance phenotype due to its independent mode of action.

We found additive (neutral) effects between pyoverdine 3G07 and ceftazidime. Given their independent modes of action—pyoverdine induces iron starvation, while ceftazidime causes cell lysis—neutral interactions between these two classes of antibacterials can be anticipated. Neutral drug interactions are beneficial from a clinical perspective because they reduce the risk that a single mutation can simultaneously confer resistance to both antibacterials (Fischbach 2011). This notion is supported by our data showing that there is hardly any overlap in high-frequency mutations between the pyoverdine and ceftazidime single treatments (Fig. 5B). However, neutral drug interactions are not necessarily making treatments evolutionarily more sustainable, as the combined drugs should not influence each other's resistance evolution (Michel et al. 2008, Bollenbach 2015). This notion is indeed supported by our data, as we found (i) similar mutational patterns in populations subjected to ceftazidime single and combo treatments (Fig. 5B), and (ii) that ceftazidime resistance became visible when pyoverdine was omitted from the combo treatment (Fig. 4).

Thus, our results show that pyoverdine cannot reduce selection for ceftazidime resistance, but it can safely be combined with it as cross-resistance is unlikely to evolve.

An important question to address is why the phenotypic signature of ceftazidime resistance is lower in the plasmid-carrying *E. coli* MGp strain compared to the naive *E. coli* MG strain (Fig. 3). We hypothesize that the metabolic burden of the multicopy plasmid (average copy number = 19) (San Millan et al. 2016) is responsible for this effect. For one thing, we show that MGp bears a baseline plasmid carriage cost (Fig. 2), which is likely associated with plasmid replication and gene expression (San Millan and MacLean 2017). On top, we argue that pyoverdine treatment amplifies these costs because DNA and protein synthesis rely on iron-containing enzymes (Messenger and Barclay 1983, Andrews et al. 2003). Hence, the dual metabolic burden could explain why evolved *E. coli* MGp populations remained more susceptible to the combo treatment than evolved *E. coli* MG populations, even though the two evolved strains exhibited similar mutational patterns regarding pyoverdine and ceftazidime resistance. While we used a multicopy plasmid containing the $bla_{\text{TEM-1}}$ gene for our experiments, we anticipate that the dual metabolic burden could similarly apply to any costly plasmid and particularly to those that require gene expression (e.g. antibiotic resistance genes) for survival in the respective environment. Overall, our findings indicate that targeting iron metabolism seems to be particularly effective for pathogens with high iron requirements.

While our previous work yielded little evidence for pyoverdine resistance evolution in several pathogens (*A. baumannii*, *S. aureus*, *K. pneumoniae*, and *P. aeruginosa*) (Vollenweider et al. 2024), we here identified a first putative target involved in partial pyoverdine resistance in *E. coli*. We found that loss-of-function mutations in the *oppABCDF* operon reduced susceptibility to pyoverdine (Fig. 6). The *oppABCDF* operon codes for a periplasmic oligopeptide importer (Davidson et al. 2008). Discovering this target of evolution surprised us because it contradicts the basic premise that pyoverdine can solely inhibit pathogens by sequestering iron extracellularly (Vollenweider et al. 2024). Accordingly, we predicted that mechanisms reducing drug entry into the cell should not be an effective resistance mechanism against pyoverdine. Now we find exactly such a mechanism to be associated with pyoverdine resistance. To reconcile this apparent discrepancy, we propose a dual mode of action of how pyoverdine can inhibit *E. coli*. The first mode of action occurs extracellularly, whereby pyoverdine chelates iron in the environment, thereby withholding it from *E. coli*. The second mode of action could involve the translocation of iron-free (apo-) pyoverdine via nonspecific importers (e.g. porins) to the periplasm and from there via nonspecific oligopeptide transporters (e.g. Opp-transporter) to the cytosol. In the cytosol, apo-pyoverdine can potentially interfere with cellular iron homeostasis. Pyoverdine is an oligopeptide (Fig. S1) and previous studies showed that the Opp transporter is nonselective towards amino acid side chains, allowing the transport of peptides of various lengths and structures (Doeven et al. 2004). Loss-of-function mutations in any of the *opp* genes could thus potentially block this second mode of action. While novel and speculative at the same time, our two modes of action model would explain why mutations in the *opp*-operon (cutting the second mode of action) only leads to partial pyoverdine resistance, given that the first mode of action remains functional. Clearly, further experiments are required to ascertain whether apo-pyoverdine is indeed translocated into *E. coli* cells and whether this mechanism is specific to *E. coli*, given the absence of similar mutational targets in other pathogens (Vollenweider et al. 2024).

In summary, we show that pyoverdine is a potent antibacterial against *E. coli* both as single treatment and in combination with the antibiotic ceftazidime. The interaction between pyoverdine and ceftazidime is neutral, both in terms of treatment efficacy and selection for resistance. While pyoverdine is evolutionary more robust than ceftazidime, pyoverdine as an adjuvant does not prevent the evolution of ceftazidime resistance. Pyoverdine treatment is particularly potent against plasmid-carrying *E. coli* strains, possibly due to a dual metabolic burden associated with plasmid maintenance. This finding suggests the pyoverdine treatment might be particularly effective against pathogens harbouring costly antibiotic-resistance plasmids.

Acknowledgments

We thank Richard Allen and Clémentine Laffont for insightful discussion, and Alvaro San Millan for providing the *E. coli* strains.

Author contributions

V.V., F.R., and R.K. designed the research; V.V. and F.R. performed the research and analysed the data; V.V., F.R., and R.K. interpreted the data; and V.V. and R.K. wrote the paper.

Supplementary data

Supplementary data is available at *FEMSML Journal* online.

Conflict of interest: None declared.

Funding

This work was supported by funding from the Swiss National Science Foundation (grant number 31003A_182499) and the University Research Priority Program (URPP) 'Evolution in Action'.

Data availability

The sequencing data for this study have been deposited in the European Nucleotide Archive (https://www.ebi.ac.uk/ena/) under accession number PRJEB80222. The raw data underlying the figures are available from the Figshare depository (https://doi.org/10.6084/m9.figshare.27045442).

References

Alekshun MN, Levy SB. Molecular mechanisms of antibacterial multidrug resistance. *Cell* 2007;**128**:1037–50.

Andrews SC, Robinson AK, Rodríguez-Quiñones F. Bacterial iron homeostasis. *FEMS Microbiol Rev* 2003;**27**:215–37.

Annamalai R, Jin B, Cao Z *et al.* Recognition of ferric catecholates by FepA. *J Bacteriol* 2004;**186**:3578–89.

Baba T, Ara T, Hasegawa M *et al.* Construction of *Escherichia coli* K-12 in-frame, single-gene knockout mutants: the Keio collection. *Mol Syst Biol* 2006;**2**:2006.0008.

Baeder DY, Yu G, Hozé N *et al.* Antimicrobial combinations: Bliss independence and Loewe additivity derived from mechanistic multihit models. *Philos Trans R Soc B Biol Sci* 2016;**371**:20150294.

Baltrus DA. Exploring the costs of horizontal gene transfer. *Trends Ecol Evol* 2013;**28**:489–95.

Bankevich A, Nurk S, Antipov D *et al.* SPAdes: a new genome assembly algorithm and its applications to single-cell sequencing. *J Comput Biol* 2012;**19**:455–77.

Barrick JE, Colburn G, Deatherage DE *et al.* Identifying structural variation in haploid microbial genomes from short-read resequencing data using breseq. *BMC Genomics* 2014;**15**:1039.

Bell G, MacLean C. The search for 'evolution-proof' antibiotics. *Trends Microbiol* 2018;**26**:471–83.

Bolger AM, Lohse M, Usadel B. Trimmomatic: a flexible trimmer for Illumina sequence data. *Bioinformatics* 2014;**30**:2114–20.

Bollenbach T. Antimicrobial interactions: mechanisms and implications for drug discovery and resistance evolution. *Curr Opin Microbiol* 2015;**27**:1–9.

Brickman TJ, McIntosh MA. Overexpression and purification of ferric enterobactin esterase from *Escherichia coli*. Demonstration of enzymatic hydrolysis of enterobactin and its iron complex. *J Biol Chem* 1992;**267**:12350–5.

Cai SJ, Inouye M. EnvZ-OmpR interaction and osmoregulation in *Escherichia coli*. *J Biol Chem* 2002;**277**:24155–61.

Chakraborty R, Storey E, van der Helm D. Molecular mechanism of ferricsiderophore passage through the outer membrane receptor proteins of *Escherichia coli*. *Biometals* 2007;**20**:263–74.

Commo F, Bot B. nplr: n-parameter logistic regression. R package version 0.1-7. CRAN, 2016.

Davidson AL, Dassa E, Orelle C *et al.* Structure, function, and evolution of bacterial ATP-binding cassette systems. *Microbiol Mol Biol Rev* 2008;**72**:317–64.

Deatherage DE, Barrick JE. Identification of mutations in laboratory-evolved microbes from next-generation sequencing data using breseq. *Eng Anal Multicell Syst Methods Protoc* 2014;**1151**:165–88.

Doeven MK, Abele R, Tampé R *et al.* The binding specificity of OppA determines the selectivity of the oligopeptide ATP-binding cassette transporter. *J Biol Chem* 2004;**279**:32301–7.

Escolar L, Pérez-Martín J, de Lorenzo V. Coordinated repression in vitro of the divergent fepA-fes promoters of *Escherichia coli* by the iron uptake regulation (Fur) protein. *J Bacteriol* 1998;**180**:2579–82.

Fischbach MA. Combination therapies for combating antimicrobial resistance. *Curr Opin Microbiol* 2011;**14**:519–23.

Ghosh C., Sarkar P, Issa R *et al.* Alternatives to conventional antibiotics in the era of antimicrobial resistance. *Trends Microbiol* 2019;**27**:323–38.

Ginsberg AM, Spigelman M. Challenges in tuberculosis drug research and development. *Nat Med* 2007;**13**:290–4.

Hirakawa H, Nishino K, Yamada J *et al.* β-lactam resistance modulated by the overexpression of response regulators of two-component signal transduction systems in *Escherichia coli*. *J Antimicrob Chemother* 2003;**52**:576–82.

Hunt MD, Pettis GS, McIntosh MA. Promoter and operator determinants for fur-mediated iron regulation in the bidirectional fepA-fes control region of the *Escherichia coli* enterobactin gene system. *J Bacteriol* 1994;**176**:3944–55.

Klebba PE. Three paradoxes of ferric enterobactin uptake. *Front Biosci* 2003;**8**:1422–36.

Klepsch MM, Kovermann M, Löw C *et al. Escherichia coli* peptide binding protein OppA has a preference for positively charged peptides. *J Mol Biol* 2011;**414**:75–85.

Lennox JL, DeJesus E, Lazzarin A *et al.* Safety and efficacy of raltegravir-based versus efavirenz-based combination therapy in treatment-naive patients with HIV-1 infection: a multicentre, double-blind randomised controlled trial. *Lancet North Am Ed* 2009;**374**:796–806.

Li H, Durbin R. Fast and accurate short read alignment with Burrows–Wheeler transform. *Bioinformatics* 2009;**25**:1754–60.

Linton KJ, Higgins CF. The *Escherichia coli* ATP-binding cassette (ABC) proteins. *Mol Microbiol* 1998;**28**:5–13.

Livermore DM, Warner M, Jamrozy D *et al.* In vitro selection of ceftazidime-avibactam resistance in Enterobacteriaceae with KPC-3 carbapenemase. *Antimicrob Agents Chemother* 2015;**59**:5324–30.

Malenga G, Palmer A, Staedke S *et al.* Antimalarial treatment with artemisinin combination therapy in Africa. *BMJ* 2005;**331**:706–7.

Masi M, Vergalli J, Ghai I *et al.* Cephalosporin translocation across enterobacterial OmpF and OmpC channels, a filter across the outer membrane. *Commun Biol* 2022;**5**:1–10.

Masulis IS, Sukharycheva NA, Kiselev SS *et al.* Between computational predictions and high-throughput transcriptional profiling: in depth expression analysis of the OppB trans-membrane subunit of *Escherichia coli* OppABCDF oligopeptide transporter. *Res Microbiol* 2020;**171**:55–63.

Messenger AJM, Barclay R. Bacteria, iron and pathogenicity. *Biochem Educ* 1983;**11**:54–63.

Michel J-B, Yeh PJ, Chait R *et al.* Drug interactions modulate the potential for evolution of resistance. *Proc Natl Acad Sci USA* 2008;**105**:14918–23.

Monserrat-Martinez A, Gambin Y, Sierecki E. Thinking outside the bug: molecular targets and strategies to overcome antibiotic resistance. *Int J Mol Sci* 2019;**20**:1255.

Moussatova A, Kandt C, O'Mara ML *et al.* ATP-binding cassette transporters in *Escherichia coli*. *Biochim Biophys Acta BBA Biomembr* 2008;**1778**:1757–71.

Murray CJL, Ikuta KS, Sharara F *et al.* Global burden of bacterial antimicrobial resistance in 2019: a systematic analysis. *Lancet North Am Ed* 2022;**399**:629–55.

Negri M-C, Lipsitch M, Blázquez J *et al.* Concentration-dependent selection of small phenotypic differences in TEM β-lactamase-mediated antibiotic resistance. *Antimicrob Agents Chemother* 2000;**44**:2485–91.

Pettis GS, Brickman TJ, McIntosh MA. Transcriptional mapping and nucleotide sequence of the *Escherichia coli* fepA-fes enterobactin region. Identification of a unique iron-regulated bidirectional promoter. *J Biol Chem* 1988;**263**:18857–63.

R Core Team. R: a language and environment for statistical computing. Vienna: R Foundation for Statistical Computing, 2020.

Rankin DJ, Rocha EPC, Brown SP. What traits are carried on mobile genetic elements, and why?. *Heredity* 2011;**106**:1–10.

Raymond KN, Dertz EA, Kim SS. Enterobactin: an archetype for microbial iron transport. *Proc Natl Acad Sci USA* 2003;**100**:3584–8.

Rezzoagli C, Archetti M, Mignot I *et al.* Combining antibiotics with antivirulence compounds can have synergistic effects and reverse selection for antibiotic resistance in *Pseudomonas aeruginosa*. *PLOS Biol* 2020;**18**:e3000805.

Rezzoagli C, Granato ET, Kümmerli R. Harnessing bacterial interactions to manage infections: a review on the opportunistic pathogen *Pseudomonas aeruginosa* as a case example. *J Med Microbiol* 2020;**69**:147–61.

Richman DD. HIV chemotherapy. *Nature* 2001;**410**:995–1001.

Ross-Gillespie A, Gardner A, West SA *et al.* Frequency dependence and cooperation: theory and a test with bacteria. *Am Nat* 2007;**170**:331–42.

RStudio Team. RStudio: integrated development environment for R. GitHub, 2020.

Sacchettini JC, Rubin EJ, Freundlich JS. Drugs versus bugs: in pursuit of the persistent predator *Mycobacterium tuberculosis*. *Nat Rev Microbiol* 2008;**6**:41–52.

Salverda MLM, De Visser JAGM, Barlow M. Natural evolution of TEM-1 β-lactamase: experimental reconstruction and clinical relevance. *FEMS Microbiol Rev* 2010;**34**:1015–36.

San Millan A, Escudero JA, Gifford DR *et al.* Multicopy plasmids potentiate the evolution of antibiotic resistance in bacteria. *Nat Ecol Evol* 2016;**1**:1–8.

San Millan A, MacLean RC. Fitness costs of plasmids: a limit to plasmid transmission. *Microbiol Spectr* 2017;**5**. https://doi.org/10.1128/microbiolspec.mtbp-0016-2017.

Schalk IJ, Guillon L. Fate of ferrisiderophores after import across bacterial outer membranes: different iron release strategies are observed in the cytoplasm or periplasm depending on the siderophore pathways. *Amino Acids* 2013;**44**:1267–77.

Seemann T. Prokka: rapid prokaryotic genome annotation. *Bioinformatics* 2014;**30**:2068–9.

Sheidy DT, Zielke RA. Analysis and expansion of the role of the *Escherichia coli* protein ProQ. *PLoS One* 2013;**8**:e79656.

Sprouffske K, Wagner A. Growthcurver: an R package for obtaining interpretable metrics from microbial growth curves. *BMC Bioinf* 2016;**17**:172.

Suh GA, Lodise TP, Tamma PD *et al.* Considerations for the use of phage therapy in clinical practice. *Antimicrob Agents Chemother* 2022;**66**:e02071–21.

Uyttebroek S, Chen B, Onsea J *et al.* Safety and efficacy of phage therapy in difficult-to-treat infections: a systematic review. *Lancet Infect Dis* 2022;**22**:e208–20.

Ventola CL. The antibiotic resistance crisis. *Pharm Ther* 2015;**40**:277–83.

Vergalli J, Bodrenko IV, Masi M *et al.* Porins and small-molecule translocation across the outer membrane of Gram-negative bacteria. *Nat Rev Microbiol* 2020;**18**:164–76.

Vogwill T, MacLean RC. The genetic basis of the fitness costs of antimicrobial resistance: a meta-analysis approach. *Evol Appl* 2015;**8**:284–95.

Vollenweider V, Rehm K, Chepkirui C *et al.* Antimicrobial activity of iron-depriving pyoverdines against human opportunistic pathogens. *eLife* 2024;**13**. https://doi.org/10.7554/eLife.92493.1.

Wale N, Sim DG, Jones MJ *et al.* Resource limitation prevents the emergence of drug resistance by intensifying within-host competition. *Proc Natl Acad Sci USA* 2017;**114**:13774–9.

Xu L, Shao C, Li G *et al.* Conversion of broad-spectrum antimicrobial peptides into species-specific antimicrobials capable of precisely targeting pathogenic bacteria. *Sci Rep* 2020;**10**:944.

Received 23 April 2024; **revised** 18 September 2024; **accepted** 13 October 2024